Calorimetric Evidence for Polymorphous Constraints on Metastable Zr-Al Phase Formation by Mechanical Alloying

E. Ma and M. Atzmon

Department of Nuclear Engineering, The University of Michigan, Ann Arbor, Michigan 48109-2104
(Received 25 April 1991)

Metastable $Zr_{100-x}Al_x$ alloys have been formed by ball milling of elemental Zr and Al powders: supersaturated hcp solid solution for $x \leq 15$, and an amorphous phase for $x \geq 17.5$. Enthalpy-composition curves for both phases were determined by measurements of the enthalpy of transformation to equilibrium. A cusp indicating the crossover of these two curves is observed near the critical composition for amorphization. Our results indicate that phase formation by ball milling in Zr-Al is determined by polymorphous constraints and not by nucleation and growth under metastable two-phase equilibrium.

In recent years, it has been shown that amorphous alloys can be synthesized by a number of new routes in addition to the traditional rapid solidification methods [1]. Among these new approaches, ball milling of crystalline elemental powder mixtures (mechanical alloying), or of crystalline intermetallic compounds, is very attractive because it can be used to synthesize bulk material [2]. The driving forces and mechanisms governing ball-milling-induced phase transformations are still a subject of debate and many investigations. Amorphization by mechanical alloying was at first hypothesized to result from rapid quenching of local melts produced by mechanical impacts [3]. Evidence for melting during explosive equilibrium phase formation was reported in Ref. [4]. Most studies, however, suggest that solid-state processes are most likely to be responsible for vitrification [5–8]. For milling of intermetallic compounds, it is suggested that the amorphization is due to the accumulation of deformation-generated defects which raise the free energy of the compound to above that of the amorphous phase [5]. For milling of elemental powder mixtures, it has been proposed that an amorphous phase nucleates and grows by a reaction under interfacial metastable equilibrium similar to that in thin-film diffusion couples [9]. Ball milling facilitates such interdiffusion reactions by fracturing and cold-welding crystalline particles to create alternating layers with fresh interfaces, and by generating a high density of defects [6–8]. Fecht *et al.* [10] recently explained the formation of an amorphous Zr-Al phase in terms of a chemically induced catastrophic transition. They hypothesize that above a certain Al concentration, a supersaturated Zr-based solid solution becomes unstable and undergoes a polymorphous "melting" transition to a glass.

The above scenarios are illustrated using a schematic diagram of the Gibbs free energy versus overall alloy composition x as shown in Fig. 1. The diagram shows free-energy curves for a solid solution (α), an amorphous phase, and the line compounds Zr_3Al, Zr_2Al, and Zr_3Al_2. The compound free energies were obtained from Ref. [11], and we note that they lie approximately on a com-

mon tangent to the α curve. During ball milling, these equilibrium compounds do not form due to severe kinetic constraints at low milling temperatures. A uniform α phase (here a hexagonal Zr-rich solid solution) has the lowest free energy up to a concentration x', at which the α phase is in metastable equilibrium with the amorphous phase of composition x'', as determined by the common tangent construction. At $x > x'$, there exists a driving force for phase separation. If nucleation of an amorphous phase having a different composition is kinetically permitted, a metastable two-phase equilibrium will be obtained. When plotted as a function of the overall composition (Fig. 1), the average free energy of the system will then follow route 1-2-4. This is the case for metastable phase formation in diffusion-controlled thin-film reactions [1,9]. However, if the system is constrained to be homogeneous at the low milling temperatures, the stability range of the α phase (solubility of B in A) will be extended up to a critical value x^* where the free energies of the α phase and the amorphous phase are equal. Above x^*, the α phase becomes unstable with respect to the amor-
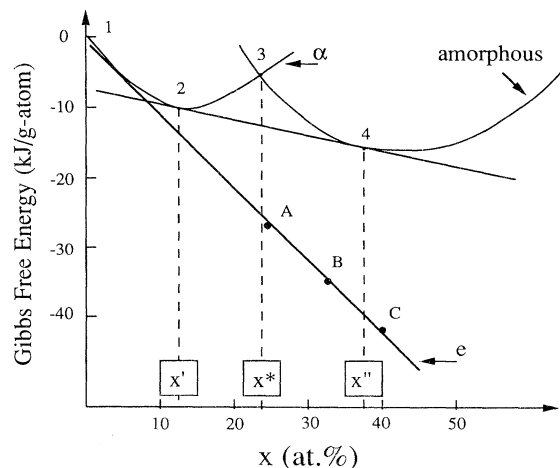

FIG. 1. Schematic free energy vs composition for several phases of a binary system (see text).

phous state and may collapse polymorphously into the amorphous phase, as proposed for Zr-Al in Ref. [10]. The free-energy versus composition curve will follow route 1-2-3-4, and a cusp will result. It is apparent from Fig. 1 and the above discussion that the driving forces and constraints which govern phase formation can be determined once the free energy of the system is characterized as a function of composition.

The present study further explores the Zr-Al system for two purposes. First, we determine experimentally, for the first time, enthalpy-composition curves for both a supersaturated metastable solid solution and an amorphous phase. Second, assuming the enthalpy to approximate the free energy for low temperatures, we use the approach outlined above to identify the constrained thermodynamics underlying metastable phase formation by ball milling.

Commercially available powders of Zr (< 180 μm, 99.9%) and Al (<44 μm, 99.9%) were alloyed in a SPEX 8000 laboratory ball mill with stainless-steel balls and vial. The ball-to-powder weight ratio was 4:1 and 8 g of mixed powder were used for each run. The Al concentration x covered a range of 0 to 30 at. %. The loaded vial was sealed in dry Ar, and a fan was used to maintain the vial temperature near $35\,^\circ$C. The milling duration ranged from 12 to 40 h, the data presented below being for 24-h milled samples. Scanning-electron-microscopy x-ray fluorescence analysis indicates that Fe and Ar impurities are present at a level below 1 and 0.5 at. %, respectively. Phases were identified by x-ray diffraction with a θ-2θ Rigaku diffractometer using Cu-$K\alpha$ radiation from a rotating-anode source operating at 7.5 kW, and by electron diffraction and transmission electron microscopy (TEM) for selected samples. Thermal analysis was performed in a differential scanning calorimeter (Perkin-Elmer DSC-7) at a heating rate of $20\,^\circ$C/min. Approximately 40 mg of milled powder were sealed hermetically in either an Al or Au pan for each DSC run. The base line was determined by repeating each run without disturbing the sample. Temperature and peak-area calibration was carried out periodically with Zn and In standards.

In agreement with Ref. [10], Zr-rich metastable $Zr_{100-x}Al_x$ alloys were obtained after 24-h ball milling. For $x \le 15$, x-ray diffractograms show all the hcp Zr peaks, broadened and consistently shifted to higher angles compared with Zr peaks for as-received powders. This indicates the formation of a Zr-based hcp solution supersaturated with Al solutes, with small grain sizes (on the order of 10 nm [10]) and reduced lattice parameters. For $x \ge 17.5$, in contrast, broad halos indicative of amorphous phase formation become the main feature in the diffraction spectra and all the crystalline Bragg peaks fade away. More convincing evidence for this qualitative difference has been found in samples heated in DSC to temperatures just below the transformation into equilibri-
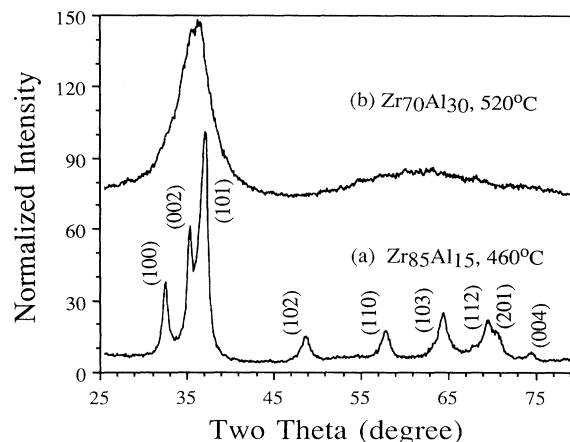

FIG. 2. X-ray-diffraction spectra for hcp $Zr_{85}Al_{15}$ solid solution and amorphous $Zr_{70}Al_{30}$ powders ball milled and annealed in DSC to $460\,^\circ$C and $520\,^\circ$C, respectively.

um compounds. Figure 2 compares the x-ray-diffraction spectra for 24-h milled $Zr_{85}Al_{15}$ and $Zr_{70}Al_{30}$ samples, annealed in DSC to $460\,^\circ$C and $520\,^\circ$C, respectively. The main features in these two spectra are the same as in corresponding as-milled samples. After annealing, grain growth occurred in the $Zr_{85}Al_{15}$ sample, giving rise to sharpened Bragg peaks, whereas the diffuse halos persisted for the $Zr_{70}Al_{30}$ sample. This rules out the possibility that the broad halos are due to nanosized crystals, since they would otherwise grow upon heating to give Bragg peaks. Selected-area diffraction patterns and high-magnification TEM observations in a $Zr_{80}Al_{20}$ sample are also consistent with the x-ray results that an amorphous phase predominates for $x \ge 17.5$. The lattice parameters of the hcp solid solution, a and c, have been determined using x-ray-diffraction data such as those in Fig. 2, curve a. A monotonic decrease in both a and c is observed as x increases all the way to $x = 15$ [12]. This result indicates that the smaller Al atoms form a substitutional solid solution with Zr. It also demonstrates that there is no obvious two-phase region (common tangent 2-4 in Fig. 1) where a solid solution with a fixed x' (hence fixed a and c) would exist before it disappears at point 4 in Fig. 1.

Figure 3 shows two typical DSC traces for 24-h milled $Zr_{87.5}Al_{12.5}$ (solid solution) and $Zr_{80}Al_{20}$ (amorphous) powders, respectively. For all our samples, heating to 600–$700\,^\circ$C resulted in only one narrow exothermic peak corresponding to the transformation into equilibrium compounds. X-ray-diffraction results indicate that in all cases the final reaction products are Zr and Zr_2Al [13]. This corresponds to the equilibrium line e in Fig. 1. The Cu_3Au-type Zr_3Al phase has not been observed, probably due to its sluggish formation kinetics [14] and the small driving force for its formation once Zr_2Al is formed (Fig. 1). Trace amounts of Zr_3Al_2 were detected only in samples with $x = 25$ and 30. Since the free energies of the
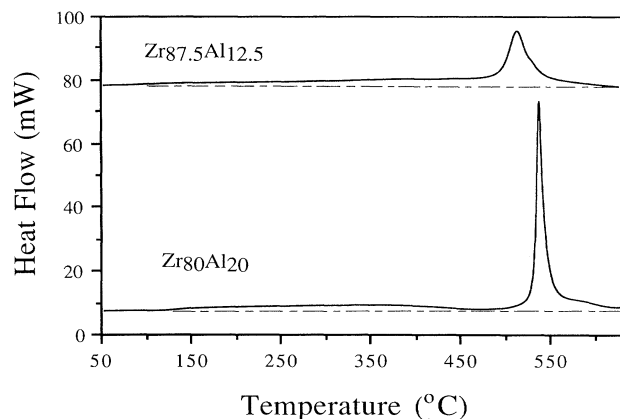
FIG. 3. DSC traces, taken at 20°C/min, for 24-h milled $Zr_{87.5}Al_{12.5}$ and $Zr_{80}Al_{20}$ powders. The narrow exothermic peak corresponds to transformation to equilibrium. The exothermic signal starts at temperatures as low as about 120°C.
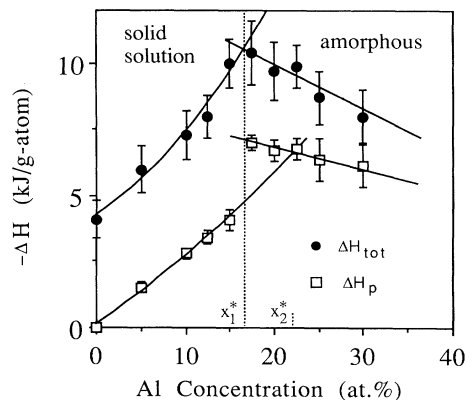

FIG. 4. Enthalpy release as a function of Al concentration for as-milled and relaxed powders during transformation to equilibrium. The dashed vertical line separates the solid solution and amorphous regions. x_1^* and x_2^* denote the cusp position for the as-milled and relaxed phases, respectively.

three compounds lie approximately on a common tangent to the α curve in Fig. 1, the free energy of transformation to equilibrium is independent of the relative amounts of these phases. It should be noted that exothermic signals start at temperatures as low as about 120°C (Fig. 3). This enthalpy release is attributable to irreversible recovery of cold-worked crystals through grain growth, defect annihilation, and strain relief, or structural relaxation in amorphous materials [15,16]. A contribution to this signal due to a reaction of trace amounts of unreacted elemental material [17] is expected to be small because the observed signal saturates with the milling time. Several reports give estimates of temperature rise induced by the kinetic energy of the milling media, ranging from 30 to 300°C [2,5,18,19]. The appreciable recovery we observe suggests a rather low ambient temperature on the order of 100°C in our experiments. The integration of the total area under the DSC trace yields the total enthalpy of the as-milled powders with respect to equilibrium, ΔH_{tot}. Since no phase transformation is detected by x-ray diffraction for samples heated up to the main DSC peak, the area under this exothermic peak corresponds to transformation enthalpy of the relaxed metastable phase to equilibrium, ΔH_p. Both ΔH_{tot} and ΔH_p as a function of Al concentration are plotted in Fig. 4, where each data point represents an average over five measurements.

A cusp, i.e., an abrupt change in slope, is observed at approximately $x = 20$ for both the ΔH_{tot} and ΔH_p curves in Fig. 4. This feature is preserved in a plot of the absolute enthalpy versus composition [12]. In the following discussion, we will use the enthalpy as an approximation to the free energy, assuming that the entropic contribution at the low milling temperatures is relatively small and will not affect the qualitative conclusions drawn below [12]. Comparing Fig. 4 with Fig. 1, it may be con-

cluded that metastable equilibrium, represented by the common tangent construction, has not been established. Rather, polymorphous constraints drive the crystalline phase out of its metastability range when the solute concentration exceeds x^*. The following kinetic route can be envisioned: Because a Zr-rich solution can form without a nucleation barrier, it forms initially and becomes richer in Al until it collapses at x^*. From Fig. 4, it appears that $x_1^* \approx 17$ for as-milled phases, and $x_2^* \approx 22$ for relaxed phases. The good agreement with the x-ray determination of $x^* \approx 17$ supports the assumption of similar behavior between free energy and enthalpy curves at low temperatures. We note from Fig. 4 that for relaxed phases, amorphization should start at $x > x_2^* = 22$. In reality, a considerable amount of enthalpy is stored in the crystalline phase (about 4.5 kJ/gatom) which raises the curve to that of ΔH_{tot} [15]. The latter crosses the relaxed amorphous curve at $x \approx 10$. However, the amorphous phase formed during milling is not in its relaxed state either. Its enthalpy curve is also raised due to a comparable amount of stored enthalpy (about 3 kJ/gatom). As a consequence, complete amorphization becomes possible at a new $x_1^* = 17$, which is observed in our experiments.

There is additional evidence indicating the absence of metastable interfacial equilibrium when some binary systems are subjected to ball milling. Homogeneous, nonequilibrium, alloy phases have been observed in systems with a nearly zero or positive heat of mixing (e.g., Cu-W [12,20], Cu-Ta [21]). In both these and the present case, the polymorphous constraints can be understood as resulting from the lack of significant mobility of both species at the low milling temperatures, and the high interfacial energy associated with phase separation in a repeatedly deformed, fine-structured alloy. Creation of a large area of such immobile interfaces would consider-

ably raise the free energy of a two-phase system and make it unstable with respect to a homogeneous phase.

Absolute enthalpy-composition curves for both the solid solution and the amorphous phases can be readily assembled with the data presented in Figs. 1 and 4. Further discussions in comparison with calculated curves will be presented separately [12]. Here we simply point out that such experimentally determined curves are very useful, especially when calculated curves, using an undercooled liquid to represent the amorphous phase, often underestimate its stability [22]. For example, no amorphous phase formation is predicted for the Zr-Al system using a calculation in Ref. [11]. In addition, our data show that the supersaturated (both as-milled and recovered) hcp solution has an enthalpy lower than that of the pure elements [12], indicating a driving force for its formation in an elemental diffusion couple [23].

In summary, we have measured, for the first time, enthalpy-composition curves for both supersaturated solid solution and amorphous phase in a binary system. The observed cusp at the crossover of these two curves near the experimental critical concentration for crystal-glass transformation (x^*) and the monotonic decrease of the lattice parameters of the solid solution phase up to x^* lend strong support to the idea that phase formation by ball milling can be determined by polymorphous constraints rather than by nucleation and growth under metastable equilibrium.

[1] W. L. Johnson, Prog. Mater. Sci. **30**, 81 (1986).

[2] For a recent review, see, for example, C. C. Koch, Annu. Rev. Mater. Sci. **19**, 121 (1989).

[3] A. E. Yermakov, E. E. Yurchikov, and V. A. Barinov, Fiz. Met. Metalloved. **52**, 1184 (1981); **54**, 935 (1982).

[4] M. Atzmon, Phys. Rev. Lett. **64**, 487 (1990).

[5] R. B. Schwarz and C. C. Koch, Appl. Phys. Lett. **49**, 146 (1986).

[6] R. B. Schwarz, R. R. Petrich, and C. K. Saw, J. Non-Cryst. Solids **76**, 281 (1985).

[7] J. Eckert, L. Schultz, and K. Urban, J. Less-Common Met. **145**, 283 (1988); G. Mazzone, A. Montone, and M. Vittori Antisari, Phys. Rev. Lett. **65**, 2019 (1990).

[8] E. Hellstern and L. Schultz, Appl. Phys. Lett. **48**, 124 (1986); J. Appl. Phys. **63**, 1408 (1988).

[9] R. B. Schwarz and W. L. Johnson, Phys. Rev. Lett. **51**, 415 (1983).

[10] H. J. Fecht, G. Han, Z. Fu, and W. L. Johnson, J. Appl. Phys. **67**, 1744 (1990).

[11] N. Saunders and V. G. Rivlin, Mater. Sci. Technol. **2**, 521 (1986); R. J. Kematick and H. F. Franzen, J. Solid State Chem. **54**, 226 (1984).

[12] E. Ma and M. Atzmon (unpublished).

[13] *Powder Diffraction File*, edited by L. G. Berry (Joint Committee on Powder Diffraction Standards, Philadelphia, 1972), No. 14-436.

[14] W. J. Meng, J. Faber, Jr., P. R. Okamoto, L. E. Rehn, B. J. Kestel, and R. L. Hitterman, J. Appl. Phys. **67**, 1312 (1990).

[15] H. J. Fecht, E. Hellstern, Z. Fu, and W. L. Johnson, Metallur. Trans. A **21A**, 2333 (1990).

[16] H. S. Chen, in *Amorphous Metallic Alloys*, edited by F. E. Luborsky (Butterworth, London, 1983), p. 169.

[17] R. B. Schwarz and R. R. Petrich, J. Less-Common Met. **140**, 171 (1988).

[18] J. Eckert, L. Schultz, E. Hellstern, and K. Urban, J. Appl. Phys. **64**, 3224 (1988).

[19] R. Schulz, M. Trudeau, J. Y. Huot, and A. Van Neste, Phys. Rev. Lett. **62**, 2849 (1989).

[20] E. Gaffet, C. Louison, M. Harmelin, and F. Faudot, Mater. Sci. Eng. A **134**, 1380 (1991).

[21] G. Veltl, B. Scholz, and H.-D. Kunze, Mater. Sci. Eng. A **134**, 1410 (1991).

[22] R. B. Schwarz, P. Nash, and D. Turnbull, J. Mater. Res. **2**, 456 (1987).

[23] E. Ma, C. V. Thompson, and L. A. Clevenger, J. Appl. Phys. **69**, 2211 (1991).